Hindawi
Mathematical Problems in Engineering
Volume 2017, Article ID 5357187, 9 pages
https://doi.org/10.1155/2017/5357187

Research Article

HRR Profiling on Integrated Radar-Communication Systems Using OFDM-PCSF Signals

Xuanxuan Tian,[1] Tingting Zhang,[1] Qinyu Zhang,[1] and Zhaohui Song[2]

[1]*Communication Engineering Research Center, Shenzhen Graduate School, Harbin Institute of Technology, Shenzhen, China*
[2]*School of Information Science and Technology, East China Normal University, Shanghai, China*

Correspondence should be addressed to Xuanxuan Tian; tianxuanxuan2008@163.com

Received 26 April 2017; Revised 23 August 2017; Accepted 6 September 2017; Published 22 October 2017

Academic Editor: Federica Caselli

In order to improve both the transmission data rate and the range resolution simultaneously in integrated radar-communication (RadCom) systems, orthogonal frequency-division multiplexing with phase-coded and stepped-frequency (OFDM-PCSF) waveform is proposed. A corresponding high resolution range (HRR) profile generation method is also presented. We first perform OFDM-PCSF waveform design by combining the intrapulse phase coding with the interpulse stepped-frequency modulation. We then give the ambiguity function (AF) based on the presented waveforms. Then, the synthetic range profile (SRP) processing to achieve HRR performance is analyzed. Theoretical analysis and simulation results show that the proposed methods can achieve HRR profiles of the targets and high data rate transmissions, while a relative low computational complexity can be achieved.

1. Introduction

Recently, the integrated radar-communication systems using orthogonal frequency division multiplexing (OFDM) signals have been popular [1, 2], where communication and radar functionalities are operated simultaneously on a single platform to improve the spectrum efficiency and cost-effectiveness. There is a large area of applications that would possibly benefit from such systems. One typical example is the intelligent transportation system, which requires both communication links among vehicles and active environment sensing capabilities. With a unified platform, all vehicles on the road could interact as a cooperative radar sensor network, which provides unique safety features and intelligent traffic routing [1]. Another example would be related to ultrawideband (UWB) radar systems for reconnaissance and navigation purposes [2]. In such networks, each sensor can perform synthetic aperture radar (SAR) imaging and ground moving target indication (GMTI) and then share it with other sensor nodes through its own communication links.

Orthogonal frequency division multiplex (OFDM) waveforms, along with coding schemes, are called multicarrier complementary phase-coded (MCPC) signals [3, 4] to enhance radar capabilities. A UWB digital system to measure the radar cross section (RCS) of targets has been proposed in [5], where the transmitted waveform is called OFDM phase-coded (OFDM-PC) signal. The OFDM-PC signals are able to minimize the peak-to-mean envelope power ratio (PMEPR). Due to the advantages on the high spectral efficiency, thumbtack-like ambiguity function (AF) [3], good Doppler tolerance [6], and flexible waveform characteristics and easy implementations [7], OFDM and its variations [7] are attractive to both academic and industrial researchers.

When considering the presented investigations related to range processing approaches in the integrated systems using traditional OFDM signals, a typical approach of direct match filtering has been presented in [2], where one-bit data is carried on each subcarrier, which results in a low data rate and high range sidelobes. An adaptive pulse compression approach to improve the detection performance has been exploited in [8]. However, a high computational effort will be introduced on the cyclic iterative algorithm. A subspace-based approach based on rotation invariance [9] and a modulation symbol-based processing approach based on element-wise division technique [1] are presented to perform range estimation, which also require high computational

complexity due to the high resolution range (HRR) performance.

To improve the transmission data rate, a subspace projection approach using the multi-OFDM chirps-based transmit pulses has been appeared in [10]. However, the approach is based on a two-dimensional parameter-searching method, which suffers from a high computational burden. To improve the data rate and range resolution, OFDM linear frequency modulation (LFM) signals based on fractional Fourier transform (FRFT) [11] and a random stepped-frequency (SF) OFDM signal based on correlation processing [12] have been given. However, both signals are prone to the range-Doppler coupling, which may lead to HRR performance degradation. An OFDM-PC strategy along with the discrete Fourier transform (DFT) and correlation processing [13] has been developed to perform range and velocity estimation. However, one of the main drawbacks for OFDM-PC signals in the radar context is that the larger instantaneous bandwidth usually follows higher sampling rate requirements, resulting in higher computational complexity.

In view of the above, we give an OFDM phase-coded stepped-frequency (OFDM-PCSF) based strategy as an improvement to [13] by combining the intrapulse (within the pulse) phase coding and interpulse (among different pulses) SF modulation. OFDM-PCSF signals can essentially synthesize the instant narrow bandwidth into effective large bandwidth, which provides improved data rate and range resolution, with low Doppler sensitivity and computational complexity. The proposed scheme, taking full advantage of the signal structure to achieve HRR performance with low computational complexity, is also provided on the receiver end.

The rest of this paper is organized as follows. The signal model of OFDM-PCSF integrated system is given in Section 2. The analysis of AF for OFDM-PCSF pulse train is presented in Section 3. The principle of SRP processing approach is explained in Section 4. The simulation results are presented in Section 5. Conclusion of the paper is given in Section 6.

2. Signal Model

2.1. Transmitted Signals. We assume that the OFDM-PCSF signals consist of a coherent burst of P pulses. The pulse repetition period is T_r. Each pulse is realized by OFDM-PC signals, which transmit on N subcarriers simultaneously. The communication messages on each subcarrier are mapped onto a sequence of M bits. Then the transmitted signals can be described as

$$x(t) = \sum_{p=0}^{P-1} s\left(t - pT_r\right) e^{j2\pi f_p t}, \tag{1}$$

where $s(t)$ is the complex envelope of OFDM-PC single pulse [13] given by

$$s(t) = \sum_{n=0}^{N-1} u_n(t)\, e^{j2\pi f_n t}, \tag{2}$$

where

$$u_n(t) = \sum_{m=0}^{M-1} a_{pnm}\,\mathrm{rect}\left(t - mt_b\right), \tag{3}$$

where $u_n(t)$ is the envelope of the phase-coded signal on the nth subcarrier, N and M are the numbers of subcarriers and chips, respectively, t_b is the chip duration, $\Delta f = 1/t_b$ is the subcarrier separation, $f_n = n\Delta f$, $\{a_{pnm}\}_{m=0}^{M-1}$ is the transmitted PC sequence on the nth subcarrier and the pth pulse, and $\mathrm{rect}(t)$ is given by

$$\mathrm{rect}(t) = \begin{cases} 1 & 0 \le t \le t_b \\ 0 & \text{otherwise.} \end{cases} \tag{4}$$

In (1), $f_p = f_c + pB$ represents the carrier frequency of the pth pulse, where f_c is the radio frequency (RF) carrier frequency and $B = N\Delta f$ is the bandwidth of the individual pulse. Therefore, the effective bandwidth of the OFDM-PCSF pulse train is $B_e = PN\Delta f$. The structure of the pulse train can be seen in Figure 1, where $T = Mt_b$ is the pulse width.

2.2. Intrapulse Phase Coding. Intrapulse phase coding begins by appropriately selecting a phase sequence of length M. An uncoded pulse width T is then divided into M equal-length intervals of t_b (chips), such that $T = Mt_b$, providing an improved range resolution.

The phase coding scheme for the construction of PC sequences is based on cyclic shifts of a phase sequence, where the transmitted messages control the cyclic-shift value. Specific construction steps are summarized as follows:

(1) Select an initial phase sequence $\mathbf{S}$ of length M with a good periodic autocorrelation function (ACF).

(2) The transmitted binary data bits $(0, +1)$ of size $(P \times N \times K)$ are generated randomly, and K is set as $2^K \le M$. The K bits data on the nth subcarrier and the pth pulse convert into the decimal form d_{pn}, which represents the time shift on the nth subcarrier and the pth pulse. The time shifts for all subcarriers and pulses are represented as $\mathbf{d} = \{d_{pn},\ p = 0, \ldots, P-1,\ n = 0, \ldots, N-1\}$.

(3) Cyclic shift of the initial phase sequence $\{a_{pnm}\}_{m=0}^{M-1} = \mathbf{S}_{\to d_{pn}}$, where $\mathbf{S}_{\to d_{pn}}$ represents cyclically shifted $\mathbf{S}$ by d_{pn}.

In order to show how the above construction works, a simple example for $P = 2,\ N = 4,\ M = 5,\ K = 2$ is shown in Table 1. The transmitted data bits are generated randomly, 5-bit Barker code is selected as the initial phase sequence, and + and − denote 1 and −1, respectively.

From Table 1, we can get that the phase coding scheme allows each subcarrier to carry K bits data and provides a signal protection mechanism, where the receiver has to know the appropriate decoding scheme to recover the transmitted data. Hence, the phase coding scheme enhances the data rate and transmission of confidentiality.

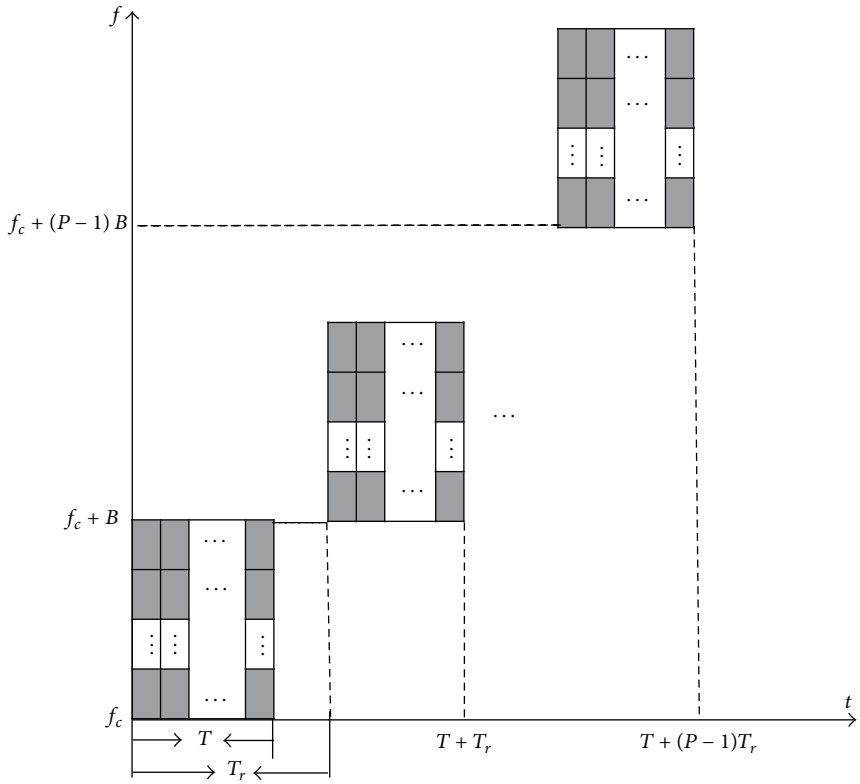

Figure 1: The structure of OFDM-PCSF pulse train.

Table 1: An example of the constructed PC sequences for $P = 2$, $N = 4$, $M = 5$, $K = 2$ and 5-bit Barker code.

Pulse	Data bits	PC sequences
1	0 0	+ + + − +
	0 1	+ + − + +
	1 1	− + + + +
	0 0	+ + + − +
2	1 1	− + + + +
	0 0	+ + + − +
	1 0	+ − + + +
	0 1	+ + − + +

3. Ambiguity Function

In this section, we discuss the AF of the proposed OFDM-PCSF signals. The equivalence of the pulse compression processing output to the AF expression is frequently used to evaluate the performance of radar signals [14]. As a consequence, the analysis on the AF of the OFDM-PCSF signals is helpful to understand how the features affect the design of the radar processing.

3.1. AF of the OFDM-PCSF Pulse Train. AF is a basic and widely applied performance metric of waveform designing and analysis in radar systems. AF is usually implemented by a matched filter bank for the detection of targets and the estimation of their ranges and velocities. It is defined as [15]

$$\chi(\tau, f_d) = \int_{-\infty}^{\infty} x(t)\, x^*(t+\tau)\, e^{j2\pi f_d t} dt, \tag{5}$$

where $*$ denotes the complex conjugate, τ and f_d represent the relative time delay and Doppler frequency of the received signal, respectively, and $x(t)$ is the reference signal for matched filtering in the receiver.

Proposition 1. *The AF of the single-pulse waveform for the OFDM-PCSF pulse train can be represented as*

$$\chi_{pc}(\tau, f_d) = \sum_{n=0}^{N-1} \sum_{q=-M+1}^{M-1} \sum_{m=0}^{M-|q|-1} a_{pnm} a^*_{pn(m+|q|)} \times \chi_r(\tau - qt_b, f_d)\, e^{j2\pi(f_d m t_b - n\Delta f \tau)}, \tag{6}$$

where

$$\chi_r(\tau, f_d) = \begin{cases} (t_b - |\tau|)\,\mathrm{sinc}\left[f_d(t_b - |\tau|)\right] e^{j\pi f_d(t_b - \tau)} & |\tau| \le t_b \\ 0 & \text{otherwise.} \end{cases} \tag{7}$$

Proof. See Appendix A. □

Table 2: Waveform parameters for the OFDM-PCSF, PCSF, and OFDM-PC signals.

Symbol	Parameter	OFDM-PCSF	PCSF	OFDM-PC
f_c	RF carrier frequency	10 GHz	10 GHz	10 GHz
P	Number of pulses	8	32	8
N	Number of subcarriers	4	0	4
M	Number of chips	5	5	5
t_b	Chip duration	1 us	1 us	1 us
T_r	Pulse repetition period	20 us	20 us	20 us
B_e	Total signal bandwidth	32 MHz	32 MHz	4 MHz
D	The size of the data	$8 \times 4 \times 2$	32×2	$8 \times 4 \times 2$

Remark 2. We consider the range AF in this paper. Hence, substituting $f_d = 0$ in (6), the range AF of the single-pulse waveform can be expressed as

$$\chi_{pc}(it_b + \kappa, 0) = (t_b - \kappa) \sum_{n=0}^{N-1} \sum_{m=0}^{M-i-1} a_{pnm} a_{pn(m+i)}^* + \kappa \sum_{n=0}^{N-1} \sum_{m=0}^{M-i-2} a_{pnm} a_{pn(m+i+1)}^*, \quad (8)$$

where $\tau = it_b + \kappa$, i is an integer, and $0 \le \kappa < t_b$.

From (6) and (8), we can see that the AF of the single-pulse waveform for OFDM-PCSF pulse train depends on the ACF of the PC sequences. The thumbtack shape is assumed to be the desirable shape of the AF. PC sequence on each subcarrier with a good periodic ACF can improve the AF performance; this also has been shown in [3]. Besides, the PC sequences with a good periodic ACF also enable us to design the radar signal processing to improve the HRR performance, which will be discussed in Section 4.

Proposition 3. *The AF of the OFDM-PCSF pulse train can be expressed as*

$$\chi(\tau, f_d) = \sum_{k=-P+1}^{P-1} e^{j2\pi((kB-f_c)\tau + (P+k-1)(kBT_r + f_d T_r - B\tau)/2)} \times \frac{\sin[\pi(P-|k|)(kBT_r + f_d T_r - B\tau)]}{\sin[\pi(kBT_r + f_d T_r - B\tau)]} \times \chi_{pc}(\tau + kT_r, f_d + kB), \quad (9)$$

where $\chi_{pc}(\cdot)$ has a similar form to (6) when $a_{pn(m+|q|)}$ is replaced with $a_{(p+|k|)n(m+|q|)}$.

Proof. See Appendix B. □

From Proposition 3, it can be seen that the AF of the OFDM-PCSF pulse train combines the properties of the AF from the OFDM-PC and SF signals. Thus, the range-Doppler coupling problem still exists due to the interpulse SF modulation.

3.2. AF Analysis. Performance analysis of the AF is evaluated by comparisons with the existing PCSF [16] and OFDM-PC signals [17]. The PCSF signals have a similar form to (1) when f_p is replaced with $f_p = f_c + p\Delta f$, and $s(t) = \sum_{m=0}^{M-1} a_{pm} \mathrm{rect}(t - mt_b)$.

The waveform parameters of the OFDM-PCSF, PCSF, and OFDM-PC signals are shown in Table 2; the 5-bit Barker code is selected as the initial phase sequence. We limit the volume computations over a subregion $\mathfrak{R} = \{|\tau| \le t_b,\ 0 \le f_d \le 1/T_r\}$; the corresponding ambiguity diagram is shown in Figure 2. Note the following observations from Figures 2(a)–2(f):

(1) The AFs of the first two signals exhibit the diagonal ridge, where a delay-Doppler coupling appears. However, the former has a relatively smaller tilt, which shows that the OFDM-PCSF signals provide reduced Doppler sensitivity compared to the PCSF signals. Besides, the simulation also demonstrates the feasibility of the OFDM-PCSF signals to realize radar-communication integration.

(2) The AF of the third signal exhibits a thumbtack, while the main-lobe width along the delay axis is much larger than the first two signals. The result demonstrates that the range resolution of the OFDM-PC signals is lower than the other two schemes, due to the fact that the bandwidth is 1/8 of the first two signals.

Hence, the OFDM-PCSF signals can provide a better HRR performance compared to the OFDM-PC signals, and the Doppler sensitivity is between the OFDM-PC and PCSF signals.

4. Synthetic Range Profile Processing

In this section, the synthetic range profile (SRP) processing approach taking full usage of the structure of the OFDM-PCSF signals is presented to achieve HRR profile. This approach is similar to the approach described in [16–18]. However, the transmitted communication messages are not considered in previous investigations.

The entire processing approach is shown in Figure 3, where the correlation processing can reduce the effects of the transmitted data on the HRR performance. Moreover, it directly operates on the transmitted and received phase codes instead of the baseband signals, providing a much lower computational complexity.

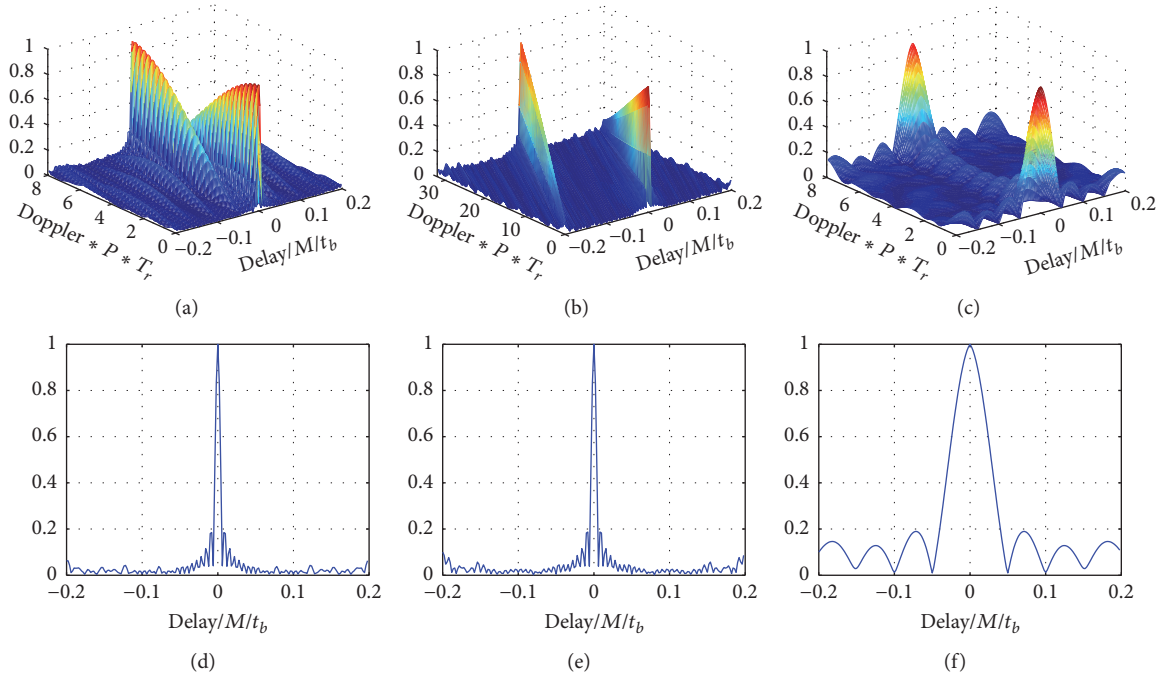

FIGURE 2: The ambiguity diagram for the different signals. (a) $\chi(\tau, f_d)$ of OFDM-PCSF; (b) $\chi(\tau, f_d)$ of PCSF; (c) $\chi(\tau, f_d)$ of OFDM-PC; (d) $\chi(\tau, 0)$ of OFDM-PCSF; (e) $\chi(\tau, 0)$ of PCSF; (f) $\chi(\tau, 0)$ of OFDM-PC.

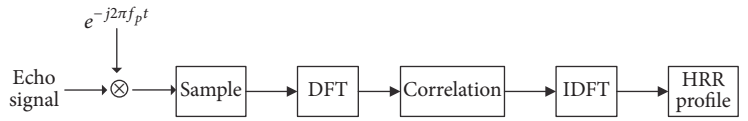

FIGURE 3: The flow chart of SRP processing approach.

Consider a point target at distance R and relative velocity v with respect to the radar. Assume that v means that the target is fleeing away from the radar and satisfies $2v/c \ll 1$, where c is the speed of light. The received echo signals in a noise-free scenario can be expressed as

$$y_r(t) = x(t-\tau), \tag{10}$$

where $\tau = 2(R - vt)/c$.

Step 1 (demodulation). The received echo signal of the pth pulse is to be demodulated by multiplying $e^{-j2\pi f_p t}$; we have

$$y(t) = \sum_{p=0}^{P-1} s(t - \tau - pT_r) e^{-j2\pi f_p \tau}. \tag{11}$$

Step 2 (sampling). The demodulated signals are to be processed in the digital domain. Therefore, we assume that the sampling frequency of the D/A converter is $f_s = N/t_b$ and sampling time is $t = pT_r + mt_b + it_b/N$, where $p = 0, \ldots, P-1$, $m = 0, \ldots, M-1$, $i = 0, \ldots, N-1$. Then the discrete form of $y(t)$ can be written as

$$y(p, m, i) = \sum_{n=0}^{N-1} a_{pnm} e^{j2\pi F_n i t_b/N} \times e^{-j2\pi(f_p + f_n)(2(R - v(pT_r + mt_b))/c)}, \tag{12}$$

where $F_n = (f_p + f_n)2v/c + f_n$.

Step 3 (DFT). Apply DFT of $y(p, m, i)$ concerning i to acquire the spectrum components of the received echo, which can be expressed as

$$Y_f(p, m, q) = \sum_{i=0}^{N-1} y(p, m, i) e^{-j2\pi iq/N} = D(p, m, q) + \varepsilon(p, m, q) \quad q = 0, \ldots, N-1, \tag{13}$$

where

$$D(p,m,q) = a_{pqm}\mathrm{Comb}(\eta) \times e^{-j2\pi(f_p+f_q)(2(R-v(pT_r+mt_b))/c)}, \tag{14}$$

$$\varepsilon(p,m,q) = \sum_{\substack{n=0\\ n\neq q}}^{N-1} a_{pnm}\mathrm{Comb}(\eta+n-q) \times e^{-j2\pi(f_p+f_n)(2(R-v(pT_r+mt_b))/c)}, \tag{15}$$

where

$$\mathrm{Comb}(\eta) = \frac{\sin(\pi\eta)}{\sin(\pi\eta/N)}e^{\pi\eta(N-1)/N}, \quad \eta = \frac{f_p t_b 2v}{c}. \tag{16}$$

From (15), $\varepsilon(p,m,q)$ means the intersubcarrier interference, which destroys the orthogonality of subcarriers. It can be negligible for the low speed targets [17]. Hence, (13) can be rewritten as

$$Y_f(p,m,q) = D(p,m,q), \tag{17}$$

which denotes the mth phased code on the nth subcarrier and the pth pulse.

Step 4 (correlation processing). To reduce the effects of the transmitted data on radar performance, performing the correlation processing between $Y_f(p,m,q)$ and $\{a_{pnm}\}$ concerning m, the resulting signal can be written as

$$Y_c(p,w,q) = \mathrm{Comb}(\eta)\,A_{pq}(w)\,e^{-j2\pi(f_p+f_q)(2(R-vpT_r)/c)} \quad |w| = 0,\ldots,M-1, \tag{18}$$

where

$$A_{pq}(w) = \sum_{m=0}^{M-|w|-1} a_{pmq}a^*_{p(m+|w|)q}e^{j2\pi(f_p+f_q)(2vmt_b/c)}, \tag{19}$$

which contains the ACF of the PC sequence $\{a_{pnm}\}_{m=0}^{M-1}$, resulting in a single peak. Hence, the peak value of $Y_c(p,w,q)$ with respect to w can be expressed as

$$Y_c(p,q) = A_{pq}\mathrm{Comb}(\eta)\,e^{-j2\pi(f_p+f_q)(2(R-vpT_r)/c)}, \tag{20}$$

where $A_{pq} = \max_w\{A_{pq}(w)\}$; this is known after PC sequence is chosen. Hence, removing A_{pq}, we get

$$Y(p,q) = \frac{Y_c(p,q)}{A_{pq}} = \mathrm{Comb}(\eta)\,e^{-j2\pi(f_c+(pN+q)\Delta f)(2(R-vpT_r)/c)}. \tag{21}$$

Setting $g = pN + q$ gives

$$Y(p,g) = \mathrm{Comb}(\eta)\,e^{-j2\pi(f_c+g\Delta f)(2(R-vpT_r)/c)} \quad g = 0,\ldots,PN-1. \tag{22}$$

Step 5 (IDFT). By performing the inverse discrete Fourier transform (IDFT) of $Y(p,g)$ concerning g, the HRR profile can be expressed as

$$y(p,l) = \frac{1}{PN}\sum_{g=0}^{PN-1} Y(p,g)\,e^{j2\pi gl/N} \quad l = 0,\ldots,PN-1, \tag{23}$$

which can be simplified to

$$y(p,l) = \frac{1}{PN}\mathrm{Comb}(\eta)\,e^{-j2\pi(f_c\tau+(\Delta f\tau-l/PN)(PN-1)/2)} \times \frac{\sin[PN\pi(\Delta f\tau - l/PN)]}{\sin[\pi(\Delta f\tau - l/PN)]}, \tag{24}$$

where $\tau = 2(R - vpT_r)/c$, $y(p,l)$ represents the HRR profile of the pth pulse, and $l = 0,\ldots,PN-1$ is the corresponding *range bin* of the IDFT output.

From (24), $|y(p,l)|$ takes maximal value at $\Delta f\tau - l/PN = h$, where h is an integer. If accumulating time is short, namely, $R \gg vpT_r$, we can get

$$R \approx \frac{[h + l/(PN)]\,c}{2\Delta f}. \tag{25}$$

From the above analysis, it can be seen that the complete processing approach can be implemented by means of DFT and IDFT operations, which makes it efficient in real time.

5. Simulation and Analysis

Simulations are carried out to demonstrate the performance of the SRP processing approach using the OFDM-PCSF signals. The details of the system parameters are summarized in Table 3. We use 13-bit Barker code and randomly generated communication data of size ($64 \times 32 \times 3$) to construct PC sequences, with additive white Gaussian noise (AWGN). The range resolution is $\Delta R = c/2B_e = 0.1465$ m, which is 1/64 of the range resolution for the OFDM-PC signals (9.3760 m).

According to Table 3, each subcarrier carries $K = 3$ bits data; the data rate can reach 0.9231 Mbps.

Firstly, simulated HRR profiles of the OFDM-PCSF signals are provided with the SRP processing and the direct match filtering [2]. We consider the two targets with $R = [2500\ \ 2500.3]$ m and $v = [10\ \ 10]$ m/s, and the corresponding HRR profile resulting from the two approaches is shown in Figure 4.

As shown in Figure 4(a), the two targets can be separated successfully and the corresponding estimated ranges are $\widetilde{R} = [2499.91\ \ 2500.23]$ m. As shown in Figure 4(b), there exists one single peak that cannot identify the two targets.

Secondly, the Doppler sensitivity characterization of the OFDM-PCSF and OFDM-PC signals using SRP processing approach is investigated. For the OFDM-PC signals, the number of subcarriers is 2048; other parameters settings are the same as in Table 3. Hence, the range resolution for both signals is the same. We consider a target with $R = 2500$ m

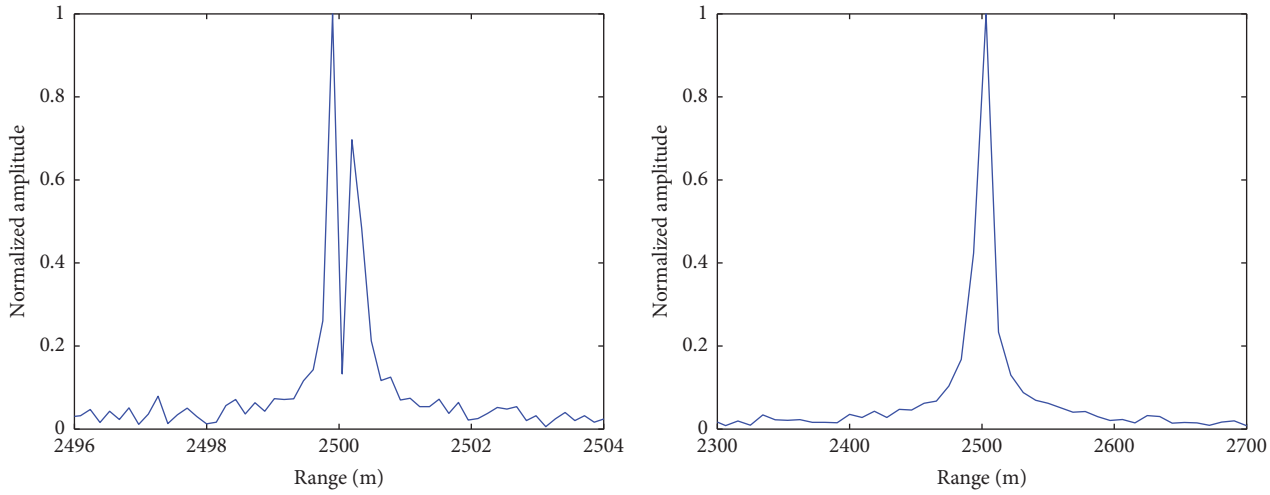

Figure 4: HRR profile of the two targets resulting from the two approaches. (a) SRP processing; (b) direct match filtering.

Table 3: OFDM-PCSF system parameters.

Symbol	Parameter	Value
f_c	RF carrier frequency	10 GHz
P	Number of pulses	64
N	Number of subcarriers	32
M	Number of chips	13
t_b	Chip duration	2 us
T	Pulse width	26 us
T_r	Pulse repetition period	104 us
δ	Pulse duty cycle	0.25
Δf	Subcarrier separation	0.5 MHz
B_e	Total signal bandwidth	1.024 GHz
SNR	Signal-to-Noise ratio	10 dB

at the different velocity $v = 0$ m/s, $v = 100$ m/s, and $v = 1000$ m/s; the corresponding HRR profile using the SRP processing approach for the different waveforms is shown in Figure 5.

As shown in Figure 5, it can be seen that velocity of the target brings the effect of HRR degradation. For $v = 100$ m/s, HRR profiles of both signals show little change that takes some translation with amplitude decline. For $v = 1000$ m/s, HRR profile of the former slips more range cells and distorts badly. After many simulations, it can be concluded that the effect of the distortion is very low for $v = 100$ m/s using both signals. However, the OFDM-PCSF signals are much more sensitive to the Doppler effects for $v = 1000$ m/s.

Hence, the OFDM-PCSF SRP processing results show that interpulse SF modulation to synthesize larger bandwidth obtains the better HRR performance. However, a cost on the Doppler sensitivity on the high speed target has to be paid. Note that, in most applications, the target speed is not so high, which makes the cost acceptable.

6. Conclusion

This paper investigates an integrated radar-communication system using OFDM-PCSF signals. The integrated waveform and associated HRR processing approach are presented to improve the transmission data rate and corresponding HRR performance. From theoretical analysis and simulation results, we can get the following observations: (i) AF demonstrates the feasibility of OFDM-PCSF signals to realize radar-communication integration and shows that the waveform can achieve HRR performance. The achieved Doppler sensitivity is between the OFDM-PC and PCSF signals. (ii) The OFDM-PCSF signals combining intrapulse phase coding scheme use the carried communication messages to control the cyclic-shift value of a phase sequence, which enables a high transmission data rate. Interpulse SF modulation can synthesize instant narrow bandwidth into effective large bandwidth, which provides improved range resolution with relatively low computation load. (iii) The SRP processing approach, taking advantage of the OFDM-PCSF signals structure, provides HRR profile of the target compared to the direct match filtering. These conclusions and presented methods can provide insights into the design and operation of typical applications of integrated radar-communication systems.

Appendix

A. Proof of Proposition 1

Substituting (2) into (5), the AF of single-pulse waveform for the OFDM-PCSF pulse train can be written as

$$\chi_{pc}(\tau, f_d) = \sum_{n=0}^{N-1} \sum_{\tilde{n}=0}^{N-1} e^{-j2\pi\tilde{n}\Delta f\tau}$$

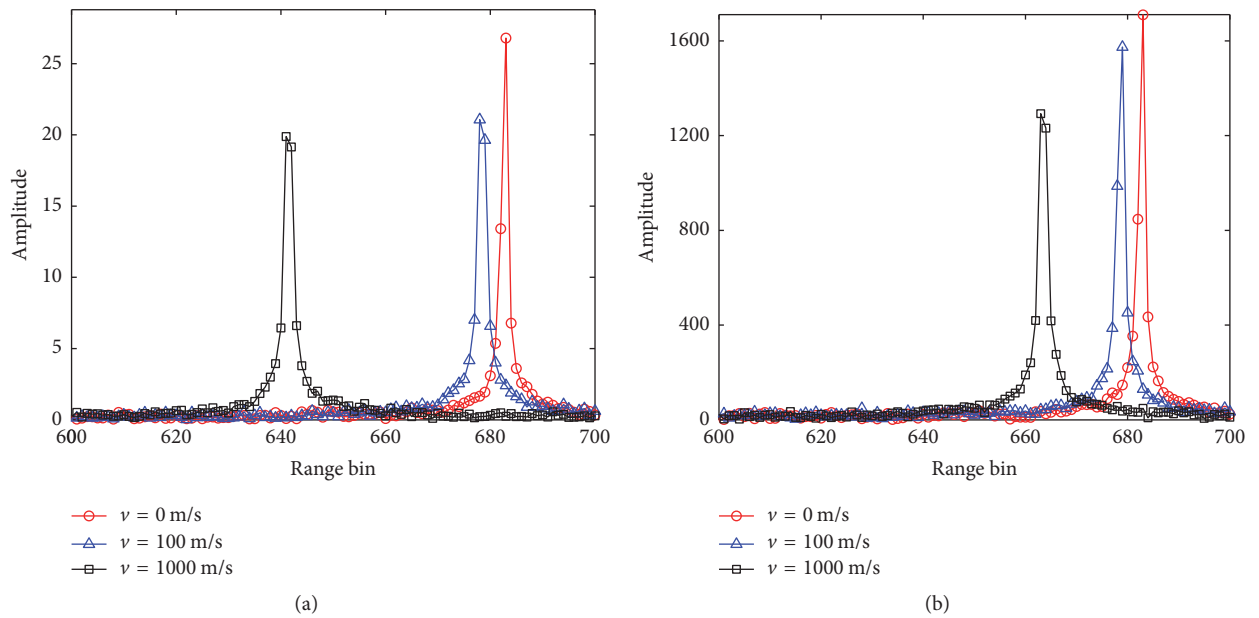

FIGURE 5: HRR profile of a target at the different velocity using SRP processing for the different waveforms. (a) OFDM-PCSF; (b) OFDM-PC.

$$\times \int_{-\infty}^{\infty} u_n(t)\, u_{\tilde{n}}^*(t+\tau)\, e^{j2\pi((n-\tilde{n})\Delta f + f_d)t} dt = \chi_m(\tau, f_d) + \chi_c(\tau, f_d), \tag{A.1}$$

where

$$\chi_m(\tau, f_d) = \sum_{n=0}^{N-1} \exp(-j2\pi n \Delta f \tau)\, \chi_n(\tau, f_d),$$
$$\chi_c(\tau, f_d) = \sum_{n=0}^{N-1} \sum_{\substack{\tilde{n}=0 \\ \tilde{n}\neq n}}^{N-1} \exp(-j2\pi \tilde{n} \Delta f \tau)\, \chi_{n,\tilde{n}}(\tau, f_d); \tag{A.2}$$

and $\chi_m(\tau, f_d)$ is main AF of $s(t)$ for $n = \tilde{n}$, $\chi_c(\tau, f_d)$ is the cross AF of $s(t)$ for $n \neq \tilde{n}$, which is regarded as the subcarrier interference, $\chi_n(\tau, f_d)$ is the auto AF of $u_n(t)$, and $\chi_{n,\tilde{n}}(\tau, f_d)$ is the cross AF of $u_n(t)$ and $u_{\tilde{n}}(t)$. Since the energy of AF is mainly concentrated on main lobe, we have

$$\chi_{pc}(\tau, f_d) = \chi_m(\tau, f_d). \tag{A.3}$$

We rewrite (3) as follows:

$$u_n(t) = \text{rect}(t) \otimes a(t), \tag{A.4}$$

where $\otimes$ is the convolution operator, $a(t) = \sum_{m=0}^{M-1} a_{pnm} \delta(t - mt_b)$, and $\delta(\cdot)$ is the Dirac function.

The AF of rect(t) can be written as

$$\chi_r(\tau, f_d) = \int_{-\infty}^{\infty} \text{rect}(t)\, \text{rect}^*(t+\tau)\, e^{j2\pi f_d t} dt = (t_1 - t_0)\, \text{sinc}[f_d(t_1 - t_0)]\, e^{j\pi f_d (t_1 + t_0)}, \tag{A.5}$$

where $t_0 = \max\{0, -\tau\}$, $t_1 = \min\{t_b, t_b - \tau\}$, and $\text{sinc}(x) = \sin(\pi x)/(\pi x)$. Then, (A.5) can be simplified to

$$\chi_r(\tau, f_d) = \begin{cases} (t_b - |\tau|)\, \text{sinc}[f_d(t_b - |\tau|)]\, e^{j\pi f_d (t_b - \tau)} & |\tau| \le t_b \\ 0 & \text{otherwise.} \end{cases} \tag{A.6}$$

The AF of $a(t)$ can be represented as

$$\chi_a(\tau, f_d) = \int_{-\infty}^{\infty} a(t)\, a^*(t+\tau)\, e^{j2\pi f_d t} dt, \tag{A.7}$$

which can be simplified to

$$\chi_a(qt_b, f_d) = \begin{cases} \sum_{m=0}^{M-|q|-1} a_{pnm} a_{pn(m+|q|)}^* e^{j2\pi f_d m t_b} & q \le |M-1| \\ 0 & \text{otherwise.} \end{cases} \tag{A.8}$$

Applying relationship (A.4) gives the following expression of $\chi_n(\tau, f_d)$:

$$\chi_n(\tau, f_d) = \chi_r(\tau, f_d) \otimes_\tau \chi_a(\tau, f_d) = \sum_{q=-M+1}^{M-1} \chi_r(\tau - qt_b, f_d)\, \chi_a(qt_b, f_d). \tag{A.9}$$

Substituting (A.9) into (A.3), we get the expression of $\chi_{pc}(\tau, f_d)$. The proof is thus complete.

B. Proof of Proposition 3

Substituting (1) into (5), the AF of the OFDM-PCSF pulse train can be written as

$$\begin{aligned}\chi(\tau, f_d) &= \int_{-\infty}^{\infty} \sum_{p=0}^{P-1} s(t - pT_r)\, e^{j2\pi f_p t} \\ &\times \sum_{\widetilde{p}=0}^{P-1} s^*\left(t + \tau - \widetilde{p}T_r\right) e^{-j2\pi f_{\widetilde{p}}(t+\tau)} e^{j2\pi f_d t} dt \\ &= \sum_{p=0}^{P-1} \sum_{\widetilde{p}=0}^{P-1} e^{j2\pi p^2 BT_r} e^{j2\pi f_d p T_r} \times e^{-j2\pi \widetilde{p} B(pT_r+\tau)} e^{-j2\pi f_c \tau} \\ &\times \chi_{pc}\left[\tau + (p - \widetilde{p})\, T_r, f_d + (p - \widetilde{p})\, B\right].\end{aligned} \tag{B.1}$$

Substituting $k = p - \widetilde{p}$ into (B.1), we can get the expression of (9). The proof is thus complete.

Conflicts of Interest

The authors declare that they do not have any commercial or associative conflicts of interest in connection with the work submitted.

Acknowledgments

This work was supported by the National Natural Science Foundation of China (NSFC) (Grants nos. 61771159, 91638204, and 61525103), Guangdong Natural Science Foundation (Grant no. 2017A030313392), and Shenzhen Fundamental Research Project (Grant no. JCYJ20150930150304185).

References

[1] C. Sturm and W. Wiesbeck, "Waveform design and signal processing aspects for fusion of wireless communications and radar sensing," *Proceedings of the IEEE*, vol. 99, no. 7, pp. 1236–1259, 2011.

[2] D. Garmatyuk, J. Schuerger, Y. T. Morton, K. Binns, M. Durbin, and J. Kimani, "Feasibility study of a multi-carrier dual-use imaging radar and communication system," in *Proceedings of the 4th European Radar Conference (EURAD '07)*, pp. 194–197, October 2007.

[3] N. Levanon, "Multifrequency complementary phase-coded radar signal," *IEE Proceedings Radar, Sonar and Navigation*, vol. 147, no. 6, pp. 276–284, 2000.

[4] N. Levanon and E. Mozeson, "Multicarrier radar signal-pulse train and CW," *IEEE Transactions on Aerospace and Electronic Systems*, vol. 38, no. 2, pp. 707–720, 2002.

[5] Y. Paichard, J. C. Castelli, P. Dreuillet, and G. Bobillot, "HYCAM: A RCS measurement and analysis system for time-varying targets," in *Proceedings of the IMTC'06 - IEEE Instrumentation and Measurement Technology Conference*, pp. 921–925, Sorrento, Italy, April 2006.

[6] G. E. A. Franken, H. Nikookar, and P. Van Genderen, "Doppler tolerance of OFDM-coded radar signals," in *Proceedings of the 3rd European Radar Conference, EuRAD 2006*, pp. 108–111, Manchester, UK, September 2006.

[7] K. Huo and J. Zhao, "The development and prospect of the new OFDM radar," *Journal of Electrical Systems and Information Technology*, vol. 37, no. 11, pp. 2776–2789, 2015.

[8] M. Ruggiano, E. Stolp, and P. Van Genderen, "Multi-target performance of LMMSE filtering in radar," *IEEE Transactions on Aerospace and Electronic Systems*, vol. 48, no. 1, pp. 170–179, 2012.

[9] J.-F. Gu, J. Moghaddasi, and K. Wu, "Delay and Doppler shift estimation for OFDM-based radar-radio (RadCom) system," in *Proceedings of the IEEE International Wireless Symposium, IWS 2015*, pp. 1–4, Shanghai, China, April 2015.

[10] Y. Liu, G. Liao, Z. Yang, and J. Xu, "A super-resolution design method for integration of OFDM radar and communication," *Journal of Electrical Systems and Information Technology*, vol. 38, no. 2, pp. 425–433, 2016.

[11] K. C. Chen, Y. L. Liu, and W. Z. Zhang, "Study on integrated radar-communication signal of OFDM-LFM based on FRFT," in *Proceedings of the IET International Radar Conference 2015*, pp. 1–6, Hangzhou, China.

[12] H. Lou, Y. Wu, Z. Ma, X. Zhao, and Q. Zhang, "A novel signal model for integration of radar and communication," in *Proceedings of the 2016 IEEE International Conference on Computational Electromagnetics (ICCEM)*, pp. 14–16, Guangzhou, China, Feburary 2016.

[13] X. Tian and Z. Song, "On radar and communication integrated system using OFDM signal," in *Proceedings of the 2017 IEEE Radar Conference (RadarConf17)*, pp. 0318–0323, Seattle, WA, USA, May 2017.

[14] R. F. Tigrek, W. J. A. De Heij, and P. Van Genderen, "OFDM signals as the radar waveform to solve doppler ambiguity," *IEEE Transactions on Aerospace and Electronic Systems*, vol. 48, no. 1, pp. 130–143, 2012.

[15] B. Deng, B. Sun, X. Wei, and X. Li, "Ambiguity function analysis for MCPC radar signal," in *Proceedings of the 2010 2nd International Conference on Industrial Mechatronics and Automation (ICIMA 2010)*, pp. 650–653, Wuhan, China, May 2010.

[16] M. A. Temple, K. L. Sitler, R. A. Raines, and J. A. Hughes, "High range resolution (HRR) improvement using synthetic HRR processing and stepped-frequency polyphase coding," *IEE Proceedings Radar, Sonar and Navigation*, vol. 151, no. 1, pp. 41–47, 2004.

[17] K. Huo, B. Deng, Y. Liu, W. Jiang, and J. Mao, "High resolution range profile analysis based on multicarrier phase-coded waveforms of OFDM radar," *Journal of Systems Engineering and Electronics*, vol. 22, no. 3, pp. 421–427, 2011.

[18] K. Huo, B. Deng, Y. Liu, W. Jiang, and J. Mao, "The principle of synthesizing HRRP based on a new OFDM phase-coded stepped-frequency radar signal," in *Proceedings of the IEEE 10th International Conference on Signal Processing (ICSP '10)*, pp. 1994–1998, IEEE, Beijing, China, October 2010.